HHS Public Access

Author manuscript

J Thorac Cardiovasc Surg. Author manuscript; available in PMC 2019 December 01.

Published in final edited form as:

J Thorac Cardiovasc Surg. 2018 December ; 156(6): 2112–2120.e2. doi:10.1016/j.jtcvs.2018.05.095.

Aortic-valve mediated wall shear stress is heterogeneous and predicts regional aortic elastic fiber thinning in bicuspid aortic valve-associated aortopathy

Emilie Bollache, PhD[1,*], **David G. Guzzardi, BSc**[2,*], **Samaneh Sattari, MSc**[3], **Katherine E. Olsen, BEng**[3], **Elena S. Di Martino, PhD**[4], **S. Chris Malaisrie, MD**[5], **Pim van Ooij, PhD**[6], **Jeremy Collins, MD**[1], **James Carr, MD**[1], **Patrick M. McCarthy, MD**[5], **Michael Markl, PhD**[1,7], **Alex J. Barker, PhD**[1], and **Paul W.M. Fedak, MD, PhD**[2,5]

[1]Department of Radiology, Feinberg School of Medicine, Northwestern University, Chicago, IL USA [2]Department of Cardiac Sciences, Cumming School of Medicine, University of Calgary, Libin Cardiovascular Institute, Calgary, AB Canada [3]Graduate Program in Biomedical Engineering, University of Calgary, Calgary, AB Canada [4]Department of Civil Engineering, Schulich School of Engineering University of Calgary, Libin Cardiovascular Institute, Calgary, AB Canada [5]Division of Surgery-Cardiac Surgery, Northwestern University, Bluhm Cardiovascular Institute, Chicago, IL USA [6]Department of Radiology, Academic Medical Center, Amsterdam, the Netherlands [7]Department of Biomedical Engineering, McCormick School of Engineering, Northwestern University, Chicago, IL USA

Abstract

Objectives—To investigate an association between the magnitude of flow-mediated aortic wall shear stress (WSS) and medial wall histopathology in bicuspid aortic valve (BAV) patients with aortopathy.

Methods—BAV patients (n=27; 52±15 years; 3 women; proximal thoracic aorta diameters = 4.4±0.7 / 4.6±0.5 cm) undergoing prophylactic aortic resection received pre-operative 4D flow MRI to quantify WSS relative to a population of healthy age- and gender-matched tricuspid aortic valve controls (n=20). Quantitative histopathology was conducted on BAV aorta tissue samples resected at surgery (n=93), and correlation was performed between elastic fiber thickness and *in vivo* aortic WSS as continuous variables. Validation of elastic fiber thickness was achieved by

Corresponding author Paul W.M. Fedak, MD PhD FRCSC, Section of Cardiac Surgery, Department of Cardiac Sciences, Cumming School of Medicine, University of Calgary, Room 880, 1403-29 Street NW, Calgary, Alberta, Canada, T2N 2T9, Phone: (403) 944-5931 / Fax: (403) 270-3715, paul.fedak@gmail.com.

*E.B. and D.G.G. share co-first authorship

Conflict of interest statement

The authors have no conflict of interest to disclose.

IRB: REB17-0207 (Oct 6, 2016)

correlation relative to tissue stiffness as determined by biaxial biomechanical testing (n=22 samples).

Results—Elastic fibers were thinner and WSS was higher along the greater curvature as compared to other circumferential regions (vs. anterior wall: p=0.003 and p=0.0001, respectively; lesser curvature: both p=0.001). Increased regional WSS was associated with decreased elastic fiber thickness (r=−0.25, p=0.02). Patient stratification with sub-analysis showed an increase in the correlation between WSS and histopathology with aortic valve stenosis (r=−0.36, p=0.002) and smaller aortic diameters (<4.5 cm: r=−0.39, p=0.03). Elastic fiber thinning was associated with circumferential stiffness (r=−0.41, p=0.06).

Conclusions—For patients with BAV, increased aortic valve-mediated WSS is significantly associated with elastic fiber thinning, particularly with aortic valve stenosis and in earlier stages of aortopathy. Elastic fiber thinning correlates with impaired tissue biomechanics. These novel findings further implicate valve-mediated hemodynamics in the progression of BAV-aortopathy.

Keywords

bicuspid aortic valve; aortopathy; wall shear stress; 4D flow MRI

Introduction

Bicuspid aortic valve (BAV) is a common congenital cardiac malformation, affecting roughly 1–2% of the population(1). One third of BAV patients may develop serious complications leading to increased morbidity including aortic aneurysms with dissection or rupture(1). Over half of patients with BAV will require a medical or surgical intervention within 20 years of diagnosis(2). The mechanisms underlying BAV-aortopathy remain unclear, and its probability of development and progression for individual patients is difficult to predict. There remains controversy regarding timing, type and extent of surgery that should be performed for bicuspid aortopathy and poor compliance with practice guidelines(3). Expert consensus has also been variable; 10 different surgical guidelines were published between 1998 and 2014(4). Together with the doubling of BAV surgical interventions over the last decade at an estimated cost of over one billion USD(5), an improved understanding of BAV-aortopathy is needed.

Despite widespread assumption that BAV-related aortic wall remodeling is associated with an underlying genetic connective tissue defect, increasing evidence also implicates abnormal valve-mediated hemodynamics of the ascending aorta in BAV-aortopathy progression(6). Phase-contrast MRI with three-dimensional (3D) velocity encoding and resolution over time (cine) along the cardiac cycle (known as ‘4D flow MRI’), has emerged as a powerful non-invasive imaging technique to investigate complex 3D proximal aorta blood flow patterns(7). Altered valve-mediated flow can increase wall shear stress (WSS), which represents the tangential viscous force exerted by blood flow on the arterial wall. WSS is a known trigger of outward vascular remodeling via endothelial mechanotransduction and may become a useful hemodynamic biomarker of BAV-aortopathy risk and severity(8). Non-invasive 4D flow MRI showed increased valve-mediated WSS in patients with normally functioning BAV as compared to patients with a tricuspid aortic valve (TAV)(9). This indicates that all

BAV patients have altered proximal aortic valve-mediated hemodynamics which may mediate the associated aortopathy.

We recently documented more severe medial elastic fiber degradation in resected aortic tissue from regions of increased WSS as compared to adjacent regions of normal WSS in the same aortae of 20 BAV patients(10). This observation supports 4D flow MRI of valve-mediated hemodynamics as a non-invasive method to identify aortic tissue at risk for aortopathy progression. However, our past work was limited by analyzing only two adjacent aortic tissue regions (although many were collected) for each patient and WSS was analyzed as a categorical variable (increased WSS: “hot” versus normal: “cold” regions). We present a more comprehensive study exploring the relationship in BAV between valve-mediated hemodynamics and aortic wall histopathology using WSS as a continuous variable and by investigating the influence of key patient-specific factors on this relationship. Metrics of histopathology were further validated by assessing biomechanical tissue stiffness.

Materials and methods

Study population

Informed consent was obtained for 27 BAV patients receiving ascending aortic surgery between January 2012 and July 2015. Patients were prospectively recruited to undergo pre-operative MRI and aortic tissue resection during surgery with Institutional Review Board (IRB) approval. Pre-operative continuous-wave Doppler ultrasound was used to classify severity of aortic valve stenosis (AS) by systolic peak velocity (mild: 2–3m/s; moderate-severe: ≥ 3m/s), and aortic regurgitation (AR) by regurgitant fraction (mild: <30%; moderate-severe: ≥ 30%)(11). Additionally, a control group of 20 healthy (non-surgical) volunteers with normal TAV and aorta was randomly identified to match the patient group for age and gender from a local 4D flow MRI database of 1673 subjects, including 105 healthy volunteers, via IRB-approved retrospective chart review with a consent waiver.

Aortic tissue collection

Aortic tissue samples (n=93) were collected during surgery as before(10), and classified according to their longitudinal and circumferential location. The ascending aorta between the level of the inferior border of the right pulmonary artery and the proximal takeoff of the brachiocephalic artery was equally divided in two, to define the proximal (AA_{prox}) and distal (AA_{dist}) ascending aortic longitudinal zones (Figure 1a). Each zone was subdivided into four circumferential regions: the anterior (A) and posterior (P) walls, as well as the greater (GC) and lesser (LC) curvatures (Figure 1b).

Histopathology: elastic fiber architecture

Circumferential Verhoeff-Van Gieson histological staining of each tissue sample and analysis of elastic fiber architecture was performed as previously described(10,12). All analyses were conducted using fiber elastic thickness as the continuous variable.

Tensile mechanical testing: tissue stiffness

To validate elastic fiber thickness as an aortopathy metric, all samples of resected bicuspid aorta tissue of sufficient size (approximately $1cm^2$; n=22, collected as above) from each aortic region of the 27 BAV patients were subjected to biaxial mechanical testing(13). Results were correlated to elastic fiber thickness. Given its putative role in aortopathy pathogenesis(14), circumferential maximum tangential stiffness of the samples was computed. Testing details, analysis and modeling of the experimental data are provided in the Supplementary Material.

MRI acquisitions: aortic wall shear stress quantification

All patient and control MRI exams were performed between 2011 and 2016. Standard-of-care thoracic exam acquisition in patients included electrocardiogram (ECG)-gated 2-dimensional cine balanced steady-state free precession images covering the left ventricle for stroke volume and ejection fraction evaluation, and at the aortic valve for Sievers BAV morphology classification(15). Additionally, contrast-enhanced MR angiography of the thoracic aorta was used to calculate aortic diameters at the sinuses of Valsalva, sinotubular junction, mid-ascending aorta, as well as proximal and distal arch to classify patients according to the Stanford-Fazel BAV-aortopathy clusters(16). Finally, a prospective ECG- and respiratory navigator-gated aortic 4D flow MRI was performed in all patients and controls to derive WSS. Details regarding MRI acquisition parameters and data analysis are provided in the Supplementary Material.

Briefly, after conventional preprocessing of each 4D flow MRI dataset and segmentation of the 3D aortic volume (Supplementary Material), peak systole was automatically detected as the frame with the highest velocity averaged over the whole volume. Peak systolic WSS vectors were then calculated throughout the entire 3D aortic surface as blood dynamic viscosity multiplied by the velocity spatial gradient at the wall(17). Local median WSS magnitude was extracted in regions of interest matched to the wall location of resected BAV tissue samples. An in-house Matlab (MathWorks, Natick, MA, USA) interface provided aortic WSS map visualization in the 3 main orientations (sagittal, coronal, axial) superimposed to magnitude anatomical images, drawing of regions of interest in any view along with real-time adjustment in the two other orthogonal views, to define the AA_{prox} and AA_{dist} longitudinal zones and A, P, GC and LC circumferential regions (Figure 1).

Statistical analysis

Lilliefors test was used to assess whether data was normally distributed. Data are reported as mean±standard deviation when normally distributed, or as median (interquartile range) otherwise. The Wilcoxon rank-sum test was used to assess differences in elastic fiber thickness, WSS between aortic regions and differences between BAV patients and healthy volunteers, as well as stratification between patient groups according to AS and aortic diameters. Associations between elastic fiber thickness, WSS and tissue stiffness were correlated, and Pearson correlation coefficients r are reported. Statistical analyses were performed using Matlab (MathWorks, Natick, MA, USA); $p<0.05$ was considered statistically significant. Funding sources played no part in data analysis or interpretation.

Results

Study Cohort

Patient demographics and pre-operative characteristics are summarized in Table 1. Twenty-six of the 27 BAV patients (96%) had either AS and/or AR: while one patient had neither, the remaining six patients without significant AS had moderate-severe AR (predominant AR), and the remaining eight patients without significant AR had moderate-severe AS (predominant AS). Healthy age- and gender-matched controls (n=20; 2 women; age: 48±14 years; weight: 95±19 kg; height: 175±5 cm) provided a physiologic normal range of WSS values.

Histopathology

A median number of three (range: 1–11) aortic tissue samples were collected in BAV patients from the tubular ascending aorta (as limited by the extent of surgical resection), yielding a total of n=93 samples (Table S1). Most samples (n=81) were collected within the proximal ascending aorta (AA_{prox}), which was resected in all but one patient. Given the lower number of samples collected in the distal ascending aorta (AA_{dist}; n=12), further results are presented over the entire ascending aorta (i.e. AA_{prox} + AA_{dist}). Elastic fiber thickness could not be assessed with histology in n=3 samples (longitudinal zone-circumferential region: AA_{prox}-A, n=1; AA_{prox}-P, n=2) due to the small size of these samples. Figure 2 provides indices of elastic fiber thickness averaged over the 27 BAV patients in the remaining samples, according to circumferential region. Medial elastic fibers were significantly thinner in the greater curvature as compared to the anterior wall (p=0.003) and lesser curvature (p=0.001; Table 2). Stratification by valve dysfunction or aortic size found no differences in severity of elastic fiber histopathology (Table 2).

4D flow MRI-derived regional aortic WSS

4D flow MRI was successfully acquired in all 27 pre-operative BAV patients and 20 healthy volunteers. Aortic WSS was calculated in all regions where BAV aortic tissue samples were collected: across all four circumferential regions in all AA_{prox} and AA_{dist} longitudinal zones, as well as in all corresponding regions for each control. Median aortic WSS on the greater curvature of healthy volunteers was significantly lower than on the lesser curvature (p=0.04; Table 2 and Figure 3). It was significantly increased in BAV patients compared to the lesser curvature and anterior wall on both the greater curvature (p=0.001 and p=0.0001, respectively; Table 2 and Figure 3) and posterior wall (p=0.003 and p=0.0006, respectively; Table 2 and Figure 3). Comparing the two groups, BAV patients had significantly higher aortic WSS than healthy volunteers at all locations except the lesser curvature (A: p=0.002; P: p=0.0001; GC: p=0.0001; Table 2 and Figure 3). Stratification of BAV patients for median aortic WSS by AS or diameter revealed no significant differences between subgroups (Table 2).

Relationship between histopathology and WSS

A significant inverse relationship was observed between elastic fiber thickness and WSS (r=-0.25, p=0.02; Figure 4a, over all locations); increased WSS was associated with decreased elastic fiber thickness.

The effects of AS and aortic diameter on the relationship between elastic fiber thickness and median WSS in BAV patients are presented in Figure 4b–c. The association was stronger in subgroups of patients with predominant AS (r=−0.36, p=0.002; Figure 4b) and smaller aortic diameter (<4.5 cm: r=−0.39, p=0.03; Figure 4c) as compared to correlation including all BAV study patients. No significant associations between elastic fiber thickness and WSS were obtained in the absence of AS or with larger aortic diameters (4.5–5 and ≥5 cm subgroups).

Validation of elastic fiber thickness with biomechanical testing of tissue stiffness

Biaxial mechanical testing of resected BAV aortic wall specimens revealed a strong trend between circumferential tissue stiffness and a decrease in elastic fiber thickness (r=−0.41, p=0.06; Figure 5).

Discussion

Elastic fiber fragmentation in the aortic media is a hallmark of bicuspid aortopathy, leading to compromised aortic biomechanics, and ultimately, catastrophic dissection and rupture(1). Understanding the mechanisms underlying maladaptive outward aortic remodeling is crucial to risk stratification and individualized surgical management strategies. Recent studies implicate aberrant valve-mediated hemodynamics in the progression of BAV-aortopathy(9,10,18,19), but its exact role in mediating histopathology and biomechanical changes remains unclear.

This novel study directly compares the magnitude of *in vivo* valve-mediated WSS in the proximal thoracic aorta with quantitative histopathology of BAV-aortopathy patients. In a large dataset of 93 tissue samples from 27 patients, we observe that: (1) the magnitude of both regional WSS and elastic fiber disruption is heterogeneous within an individual BAV patient’s aorta; (2) aortic WSS correlates with regional elastic fiber thinning; (3) the association between WSS and regional histopathology is strongest with predominant AS and in mildly-dilated aortas (<4.5cm); and (4) elastic fiber thinning correlates with impaired tissue biomechanics.

Outward vascular remodeling can occur in response to increased WSS as an adaptive mechanism to decrease the effective WSS sensed by local endothelial cells and return regional WSS to a physiologic range(20). Importantly, we previously documented that BAV patients do not show expected decreases in regional WSS following aortic dilatation(20). Similarly, we found in the present study that WSS was significantly increased in BAV patients when compared to TAV healthy volunteers at all circumferential locations but the lesser curvature. Compared to TAV, abnormal BAV cusp architecture may preclude normalization of valve-mediated WSS despite progressive outward aortic remodeling. Consequently, BAV-aortopathy may manifest as a more severe and progressive aortopathy

than TAV patients with similar proximal aortic WSS. The present study supports, but does not confirm, a causative role for aortic WSS in the progression of BAV-aortopathy.

Valve-mediated WSS may be a particularly important trigger for pathogenesis in early stages (when the aorta is smaller) and in the presence of predominant AS. A causative role for underlying genetic connective tissue defects cannot be dismissed. Though genetic etiology continues to lack strong supporting evidence, our data may suggest that valve-mediated WSS is less important a trigger for exacerbating local histopathology in patients with predominant AR. These patients are suspected to have a genetic connective tissue defect and are more commonly younger with primarily root dilatation (root phenotype)(21,22). Importantly, our findings of an association between magnitude of WSS and severity of local histopathology are most pronounced when stratified by valve function and aortic diameter. The correlation between increased aortic WSS and decreased elastic fiber thickness is greater in BAV-AS patients than when pooling all BAV patients, and was not observed in BAV-AR patients. These findings parallel previous studies where BAV-mediated aortic hemodynamics are influenced by the type (AS or AR) and severity of valve dysfunction(18,23). Beyond hemodynamic differences, the behaviour of these two BAV populations following isolated aortic valve replacement (AVR) is dramatically different; the 10-fold higher risk of events in BAV-AR leads to its association with the malignant root phenotype of BAV-aortopathy(21,22). These findings are corroborated by demonstrably worse histopathology scoring of resected BAV-AR aortic tissue compared to BAV-AS(24,25). The latter is more stable over time, and within this BAV population the present study documents a significant inverse correlation between magnitude of WSS and histopathology. Girdauskas and colleagues(26) similarly found an association between the degree of histopathology in resected BAV-AS tissue impinged upon by the systolic jet at the aortotomy site, but not in BAV-AR samples. Together, these findings suggest that BAV-AS confers a predictable pattern of WSS-mediated regional aortopathy, and supports BAV-AS and BAV-AR aortas as discrete clinical entities with distinct mechanisms of aortopathy pathogenesis. Non-invasive WSS identification of diseased aorta may be preferable in selected BAV populations. Other non-invasive hemodynamic indices such as oscillatory shear index may best correlate in BAV-AR, and remain an important interest for exploration in future studies.

Herein, we report the strongest inverse correlation between aortic WSS and elastic fiber thickness in mildly-dilated BAV aortas (<4.5cm). Larger aneurysms may reflect more advanced disease with loss of sensitivity to obtain significant correlations in these patients. We speculate that the observation of a significant correlation between the severity of histopathology and WSS in smaller diameter aorta suggests a causative role for increased aortic WSS yielding increased elastic fiber degeneration in the early stages of disease. These data also highlight the increasing appreciation that aortic size may not always predict the risk of aortic events or aortopathy severity(27). Our data show that subgroups of BAV patients with aorta less than 4.5cm (below current resection thresholds) may have substantially increased regional WSS with more severe histopathology that 4D flow MRI can identify. Further studies are needed to determine if such patients should be screened preoperatively and have more aggressive prophylactic resection at the time of AVR. The correlation of WSS with simple histopathology for larger aortae with more advanced stages

of disease may require more robust tools for discrimination such as biomechanical energy loss(28). Our future work is aimed at such study design. We document that tissue from the greater curvature and posterior wall is subjected to increased aortic WSS as compared to the lesser curvature and anterior wall in BAV patients. Similar to others, we show elastic fiber thinning is greatest at the greater curvature(29), yet in the context of the correlations reported here and before(10), the greater curvature is not the only region to exhibit substantial aortopathy expression. These data support the emerging concept of regional heterogeneity within the BAV aorta: hemodynamics(9,18,19), smooth muscle cell origin and function(30), protease expression(10,31), oxidative stress(32) and histopathology(10,26,29). Raaz and colleagues(14) demonstrated in a murine model that regional variations in vascular remodeling may propagate aortopathy, and the present findings of regional WSS-mediated histopathological differences within the same aorta may similarly contribute to the progression of BAV-aortopathy.

Aortic dissection or rupture is prevented by healthy biomechanical properties of aortic tissue. Forsell and colleagues(33) previously documented increased collagen-related stiffness in aneurysmal BAV versus TAV aortic tissue. To validate elastic fiber thinning as a predictive biomarker of aortic disease, we investigated its relationship with the stiffness of the obtained tissue samples. Regional aortic tissue stiffness precedes aortic growth in animal models of human disease and is validated as a critical biomechanical marker of aortopathy progression(14). We report for the first time that decreased elastic fiber thickness corresponds with increased circumferential tissue stiffness in human BAV aorta. These data support elastic fiber thinning as a histopathologic biomarker of BAV-aortopathy that can be influenced by local aortic valve-mediated WSS.

Our novel findings provide two important contributions to the BAV literature. First, the correlation of *in vivo* aortic WSS with quantitative tissue histopathology severity provides unique insight into BAV-aortopathy, and supports a critical role for hemodynamics in its pathogenesis. However, we and others believe(6,34) that hemodynamics likely acts synergistically with an inherent extracellular matrix dysregulation and other cellular mechanisms. Second, we provide data to support an association between non-validated hemodynamic imaging biomarkers with validated tissue metrics of aortopathy (elastic fiber architecture and biomechanical stiffness). Long-term clinical outcomes study will be required in a larger patient cohort to validate non-invasive hemodynamic imaging biomarkers, such as WSS, as a promising tool for risk stratification and individualized resection strategies for BAV patients(35).

We cannot exclude the effects of selection bias on our analysis and conclusions. Tissue resection performed at the operating surgeon’s discretion and resection of smaller aortae may reflect unmeasured effects, such as intraoperative observations of tissue quality or thickness. Though previously examined in BAV patients(10,12), elastic fiber thickness represents the first quantitative aortopathy metric correlated to aortic WSS and biomechanical stiffness in BAV-aortopathy. However, it is possible that our methods are not sufficiently sensitive to discern subtle differences in the diffuse aortopathy of moderately- and severely-dilated aortas. Development of other quantitative indices may be needed with advanced microscopy(29). In addition, we report a moderate correlation between WSS and

elastic fiber thickness which could be attributable to spatial registration between histology and imaging whose spatial scales and resolutions differ. An association between histopathology and tissue stiffness from a small sample using biaxial mechanical testing was shown. Future studies with more comprehensive constitutive modeling of tissue biomechanics and more advanced multiple linear regression models are warranted to fully explore the relationships between *in vivo* WSS and aortic histopathology investigated in this study. Finally, longitudinal clinical study of a larger cohort, along with stratification of patients according to the severity of AS and valve morphology (Sievers classification), is needed to validate aortic WSS as a predictor of disease progression and clinically-relevant acute aortic events for discrete BAV populations.

Conclusion

Increased aortic valve-mediated WSS is associated with elastic fiber thinning in BAV patients, particularly in the presence of AS and for earlier stages of aortopathy. Elastic fiber thinning correlates with impaired tissue biomechanics. These novel findings implicate valve-mediated hemodynamics in the progression of BAV-aortopathy and encourage further validation of non-invasive hemodynamic imaging biomarkers for risk stratification and development of individualized aortic resection strategies beyond diameter alone.

Supplementary Material

Refer to Web version on PubMed Central for supplementary material.

Acknowledgments

Sources of funding: This work was supported by the National Institutes of Health grants R01HL115828 (MM), R01HL133504 (AJB, PWMF) and K25HL119608 (AJB), the American Heart Association Midwest Affiliate grant 16POST27250158 (EB), an Alberta Innovates Health Solutions MD-PhD Studentship (DGG), and by the Melman Bicuspid Aortic Valve Program, Bluhm Cardiovascular Institute (PWMF).

Glossary of Abbreviations

3D	three-dimensional
4D flow MRI	three-dimensional time-resolved phase-contrast magnetic resonance imaging with three-dimensional velocity encoding
BAV	bicuspid aortic valve
AS	aortic stenosis
AR	aortic regurgitation
AA_{prox}	proximal ascending aorta
AA_{dist}	distal ascending aorta
A	anterior wall

P	posterior wall
GC	greater curvature
LC	lesser curvature
AVR	aortic valve replacement
WSS	wall shear stress
TAV	tricuspid aortic valve

References

1. Fedak PWM, Verma S, David TE, Leask RL, Weisel RD, Butany J. Clinical and pathophysiological implications of a bicuspid aortic valve. Circulation. 2002; 106(8):900–4. [PubMed: 12186790]
2. Fedak PWM. Bicuspid aortic valve and the specialty clinic: are your patients at risk? Cardiol Young. 2017 Apr 6; 27(3):411–2. [PubMed: 28260551]
3. Verma S, Yanagawa B, Kalra S, Ruel M, Peterson MD, Yamashita MH, et al. Knowledge, attitudes, and practice patterns in surgical management of bicuspid aortopathy: a survey of 100 cardiac surgeons. J Thorac Cardiovasc Surg. 2013; 146(5):1033–1040 e4. [PubMed: 23988289]
4. Hardikar AA, Marwick TH. The natural history of guidelines: The case of aortopathy related to bicuspid aortic valves. Int J Cardiol. 2015; 199:150–3. [PubMed: 26197400]
5. Opotowsky AR, Perlstein T, Landzberg MJ, Colan SD, O'Gara PT, Body SC. , et al. J Thorac Cardiovasc Surg. Vol. 146. Elsevier Inc; 2013 Aug. A shifting approach to management of the thoracic aorta in bicuspid aortic valve; 339–46.
6. Girdauskas E, Borger MA, Secknus MA, Girdauskas G, Kuntze T. Is aortopathy in bicuspid aortic valve disease a congenital defect or a result of abnormal hemodynamics? A critical reappraisal of a one-sided argument. Eur J Cardio-Thoracic Surg. 2011; 39(6):809–14.
7. Markl M, Schnell S, Wu C, Bollache E, Jarvis K, Barker AJ, et al. Advanced flow MRI: emerging techniques and applications. Clin Radiol. 2016 Aug; 71(8):779–95. [PubMed: 26944696]
8. Tanweer O, Wilson TA, Metaxa E, Riina HA, Meng H. A Comparative Review of the Hemodynamics and Pathogenesis of Cerebral and Abdominal Aortic Aneurysms: Lessons to Learn From Each Other. J Cerebrovasc Endovasc Neurosurg. 2014; 16(4):335. [PubMed: 25599042]
9. Barker AJ, Markl M, Bürk J, Lorenz R, Bock J, Bauer S, et al. Bicuspid aortic valve is associated with altered wall shear stress in the ascending aorta. Circ Cardiovasc Imaging. 2012; 5(4):457–66. [PubMed: 22730420]
10. Guzzardi DG, Barker AJ, Van Ooij P, Malaisrie SC, Puthumana JJ, Belke DD, et al. Valve-Related Hemodynamics Mediate Human Bicuspid Aortopathy: Insights From Wall Shear Stress Mapping. J Am Coll Cardiol. 2015; 66(8):892–900. [PubMed: 26293758]
11. Nishimura RA, Otto CM, Bonow RO, Ruiz CE, Skubas NJ, JPE, et al. 2014 AHA / ACC Guideline for the Management of Patients With Valvular Heart Disease A Report of the American College of Cardiology / American Heart Association Task Force on Practice Guidelines. 2014
12. Bauer M, Pasic M, Meyer R, Goetze N, Bauer U, Siniawski H, et al. Morphometric analysis of aortic media in patients with bicuspid and tricuspid aortic valve. Ann Thorac Surg. 2002; 74(1): 58–62. [PubMed: 12118804]
13. Rosin NL, Agabalyan N, Olsen K, Martufi G, Gabriel V, Biernaskie J, et al. Collagen structural alterations contribute to stiffening of tissue after split-thickness skin grafting. Wound Repair Regen. 2016; 24(2):263–74. [PubMed: 26749086]
14. Raaz U, Zöllner AM, Schellinger IN, Toh R, Nakagami F, Brandt M, et al. Segmental aortic stiffening contributes to experimental abdominal aortic aneurysm development. Circulation. 2015; 131(20):1783–95. [PubMed: 25904646]
15. Sievers HH, Schmidtke C. A classification system for the bicuspid aortic valve from 304 surgical specimens. J Thorac Cardiovasc Surg. 2007; 133(5):1226–33. [PubMed: 17467434]

16. Kari FA, Fazel SS, Mitchell RS, Fischbein MP, Miller DC. Bicuspid aortic valve configuration and aortopathy pattern might represent different pathophysiologic substrates. J Thorac Cardiovasc Surg. 2012 Aug; 144(2):516–7. [PubMed: 22698560]
17. Potters WV, van Ooij P, Marquering H, VanBavel E, Nederveen AJ. Volumetric arterial wall shear stress calculation based on cine phase contrast MRI. J Magn Reson Imaging. 2015 Feb; 41(2):505–16. [PubMed: 24436246]
18. Bissell MM, Hess AT, Biasiolli L, Glaze SJ, Loudon M, Pitcher A, et al. Aortic dilation in bicuspid aortic valve disease: Flow pattern is a major contributor and differs with valve fusion type. Circ Cardiovasc Imaging. 2013; 6(4):499–507. [PubMed: 23771987]
19. Mahadevia R, Barker AJ, Schnell S, Entezari P, Kansal P, Fedak PWM, et al. Bicuspid aortic cusp fusion morphology alters aortic three-dimensional outflow patterns, wall shear stress, and expression of aortopathy. Circulation. 2014; 129(6):673–82. [PubMed: 24345403]
20. van Ooij P, Markl M, Collins JD, Carr JC, Rigsby C, Bonow RO, et al. Aortic Valve Stenosis Alters Expression of Regional Aortic Wall Shear Stress: New Insights From a Dimensional Flow Magnetic Resonance Imaging Study of 571 Subjects. J Am Heart Assoc. 2017 Sep 13.6(9):e005959. [PubMed: 28903936]
21. Girdauskas E, Rouman M, Disha K, Espinoza A, Misfeld M, Borger MA, et al. Aortic Dissection After Previous Aortic Valve Replacement for Bicuspid Aortic Valve Disease. J Am Coll Cardiol. 2015; 66(12):1409–11. [PubMed: 26383730]
22. Della Corte A, Bancone C, Quarto C, Dialetto G, Covino FE, Scardone M, et al. Predictors of ascending aortic dilatation with bicuspid aortic valve: a wide spectrum of disease expression. Eur J Cardio-Thoracic Surg. 2007; 31(3):397–405.
23. Shan Y, Li J, Wang Y, Wu B, Barker AJ, Markl M, et al. Aortic shear stress in patients with bicuspid aortic valve with stenosis and insufficiency. J Thorac Cardiovasc Surg. 2017 Jun; 153(6): 1263–1272.e1. [PubMed: 28268004]
24. Roberts WC, Vowels TJ, Ko JM, Filardo G, Hebeler RF, Henry AC, et al. Comparison of the structure of the aortic valve and ascending aorta in adults having aortic valve replacement for aortic stenosis versus for pure aortic regurgitation and resection of the ascending aorta for aneurysm. Circulation. 2011; 123(8):896–903. [PubMed: 21321157]
25. Girdauskas E, Rouman M, Borger MA, Kuntze T. Comparison of aortic media changes in patients with bicuspid aortic valve stenosis versus bicuspid valve insufficiency and proximal aortic aneurysm. Interact Cardiovasc Thorac Surg. 2013; 17(6):931–6. [PubMed: 24006478]
26. Girdauskas E, Rouman M, Disha K, Fey B, Dubslaff G, von Kodolitsch Y, et al. Morphologic and Functional Markers of Aortopathy in Patients With Bicuspid Aortic Valve Insufficiency Versus Stenosis. Ann Thorac Surg. 2017 Jan; 103(1):49–57. [PubMed: 27526648]
27. Coady MA, Rizzo JA, Hammond GL, Mandapati D, Darr U, Kopf GS, et al. What is the appropriate size criterion for resection of thoracic aortic aneurysms? J Thorac Cardiovasc Surg. 1997; 113(3):476–91. [PubMed: 9081092]
28. Chung J, Lachapelle K, Wener E, Cartier R, De Varennes B, Fraser R, et al. Energy loss, a novel biomechanical parameter, correlates with aortic aneurysm size and histopathologic findings. Journal of Thoracic and Cardiovascular Surgery. 2014:1082–9. [PubMed: 25129601]
29. Tsamis A, Phillippi JA, Koch RG, Chan PG, Krawiec JT, D'Amore A, et al. Extracellular matrix fiber microarchitecture is region-specific in bicuspid aortic valve-associated ascending aortopathy. J Thorac Cardiovasc Surg. 2016; 151(6):1718–1728 e5. [PubMed: 26979916]
30. Jiao J, Xiong W, Wang L, Yang J, Qiu P, Hirai H, et al. Differentiation defect in neural crest-derived smooth muscle cells in patients with aortopathy associated with bicuspid aortic valves. EBioMedicine. 2016; 10:282–90. [PubMed: 27394642]
31. Ikonomidis JS, Ruddy JM, Benton SM, Arroyo J, Brinsa TA, Stroud RE, et al. Aortic dilatation with bicuspid aortic valves: Cusp fusion correlates to matrix metalloproteinases and inhibitors. Ann Thorac Surg. 2012; 93(2):457–63. [PubMed: 22206960]
32. Kotlarczyk MP, Billaud M, Green BR, Hill JC, Shiva S, Kelley EE, et al. Regional Disruptions in Endothelial Nitric Oxide Pathway Associated With Bicuspid Aortic Valve. Ann Thorac Surg. 2016 Oct; 102(4):1274–81. [PubMed: 27283108]

33. Forsell C, Björck HM, Eriksson P, Franco-Cereceda A, Gasser TC. Biomechanical Properties of the Thoracic Aneurysmal Wall: Differences Between Bicuspid Aortic Valve and Tricuspid Aortic Valve Patients. Ann Thorac Surg. 2014 Jul; 98(1):65–71. [PubMed: 24881863]

34. Michelena HI, Prakash SK, Della Corte A, Bissell MM, Anavekar N, Mathieu P, et al. Bicuspid aortic valve identifying knowledge gaps and rising to the challenge from the international bicuspid aortic valve consortium (BAVCON). Circulation. 2014; 129(25):2691–704. [PubMed: 24958752]

35. Fedak PWM, Verma S. Bicuspid aortopathy and the development of individualized resection strategies. J Thorac Cardiovasc Surg. 2014 Nov; 148(5):2080–1. [PubMed: 25444189]

Perspective statement

For the first time in bicuspid aortopathy, we report direct correlation between quantitative in vivo aortic wall shear stress and elastic fiber histopathology. Histopathology corresponds with impaired tissue biomechanics, and implicates abnormal bicuspid aortic valve-mediated hemodynamics in aortopathy progression. Research into flow imaging for non-invasive biomarker risk stratification is warranted.

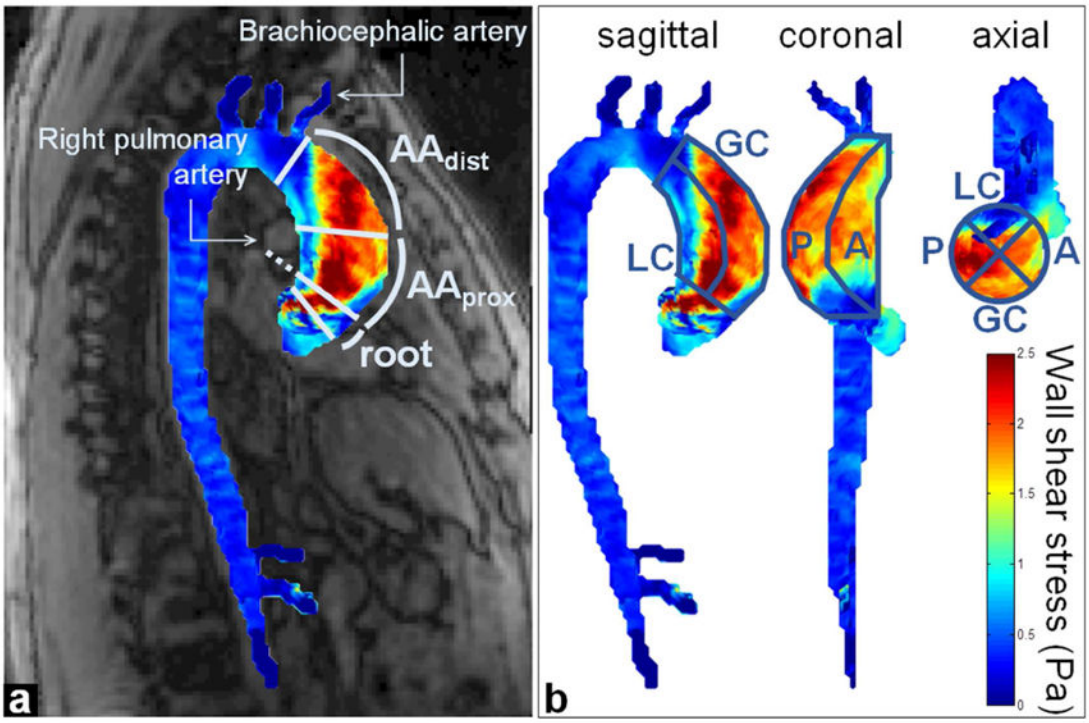

Figure 1.

Example of 4D flow MRI-derived aortic wall shear stress map in a BAV patient and definition of aortic regions of interest matching resected tissue sample location. a) Two longitudinal zones were defined as the proximal (AA_{prox}) and distal (AA_{dist}) ascending aorta, using anatomical landmarks from magnitude images (details in text). b) Circumferential regions (A: anterior; P: posterior: GC: greater and LC: lesser curvature) were defined using the sagittal, coronal and axial views.

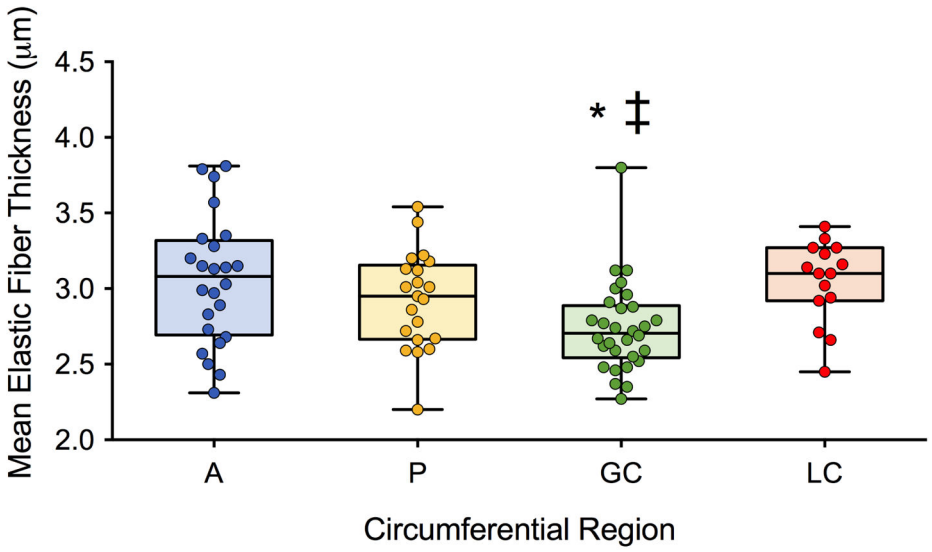

Figure 2.

Aortic elastic fiber thickness assessed using histology in BAV patients according to the circumferential location, while pooling the proximal and distal ascending aorta (A: anterior; P: posterior: GC: greater and LC: lesser curvature). Columns illustrate median values while error bars indicate interquartile ranges. *: $p<0.05$ **for comparison against A; ‡:** against LC.

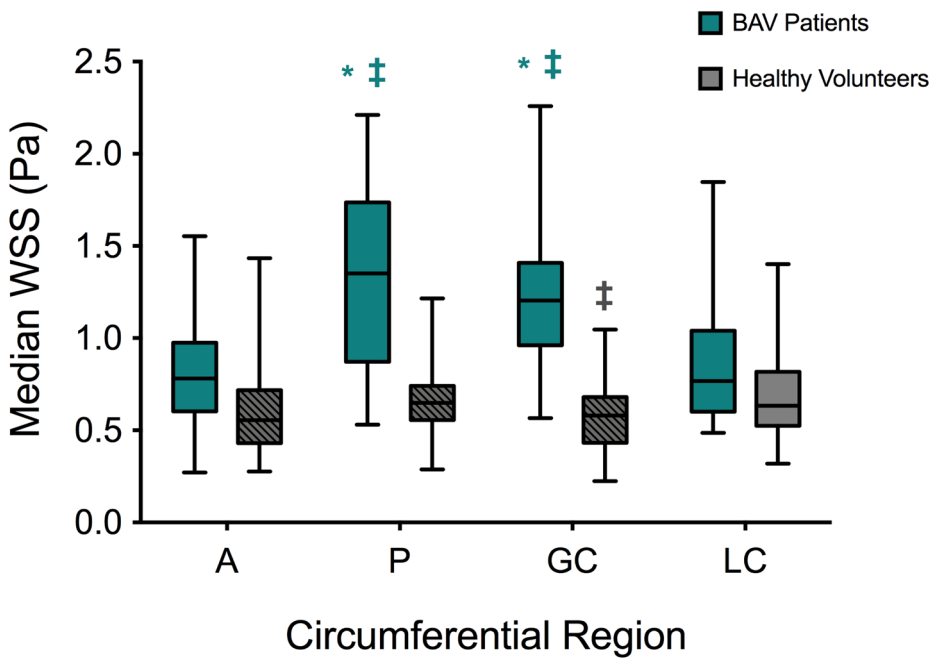

Figure 3.

Aortic wall shear stress (WSS) assessed using 4D flow MRI in BAV patients (blue) and healthy volunteers (grey) according to the circumferential location, while pooling the proximal and distal ascending aorta (A: anterior; P: posterior: GC: greater and LC: lesser curvature). Columns illustrate median values while error bars indicate interquartile ranges. Hashed regions: $p<0.05$ against BAV patients. *: $p<0.05$ for comparison against A; ‡: against LC, within each group.

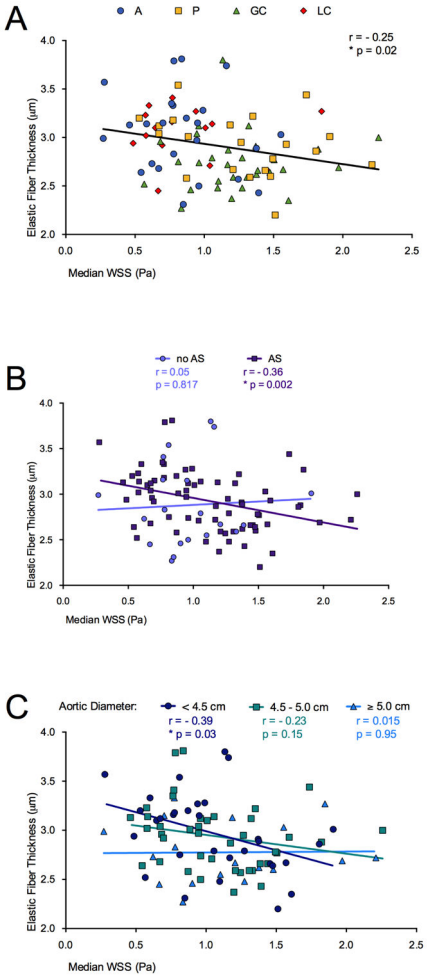

Figure 4.

Correlations for comparison between aortic elastic fiber thickness and wall shear stress (WSS): a) over all patients and all locations (A: anterior; P: posterior: GC: greater and LC: lesser curvature); b) in patients with aortic valve stenosis (AS, squares); c) in longitudinal ascending aortic locations with a diameter <4.5 cm (circles). Correlation coefficients r, p-values and lines of best fit are provided.

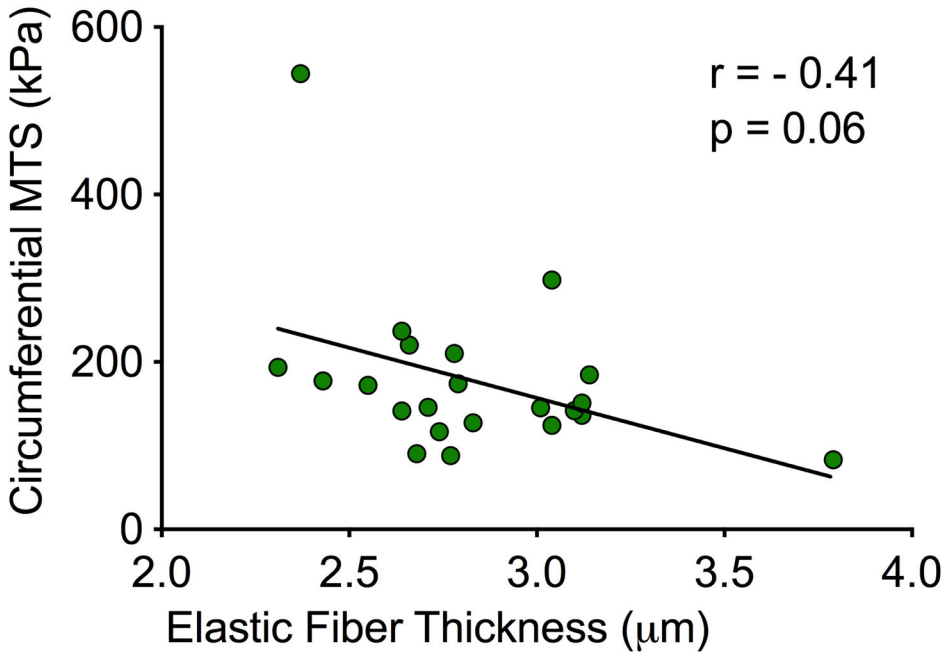

Figure 5.
Correlations for comparison between aortic elastic fiber thickness and circumferential maximum tangential stiffness (MTS). Correlation coefficient r, p-values and line of best fit are provided.

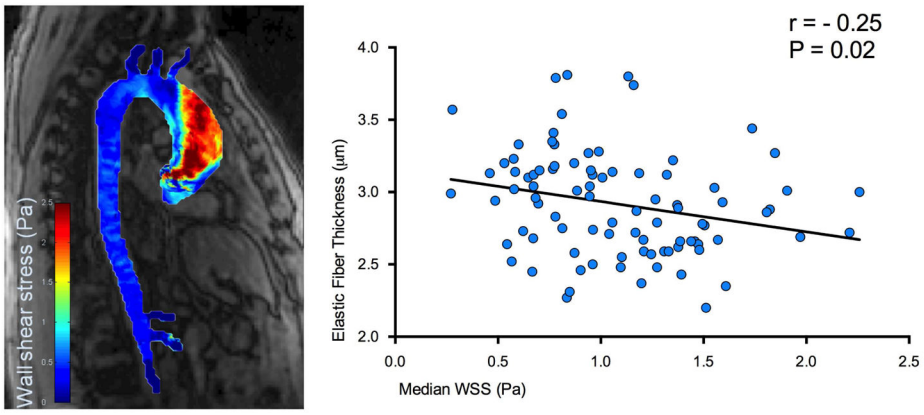

Figure 6. Central picture

In vivo wall shear stress correlates with local elastic fiber thinning in the BAV aorta.

Table 1

BAV patient pre-operative characteristics.

	BAV Patients
Pre-operative characteristics	(n=27)
Women, n (%)	3 (11)
Age (years), mean±SD	52±15
Weight (kg), mean±SD	89±17
BSA (m^2), mean±SD	2.09±0.24
Sievers BAV classification	
type 0 - ap, n (%)	0 (0)
type 0 - lat, n (%)	3 (11)
type 1 - RL, n (%)	14 (52)
type 1 - RN, n (%)	2 (7)
type 1 - LN, n (%)	1 (4)
type 2 - RL/RN, n (%)	7 (26)
AS: none/mild/mod-sev, n (%)	7 (26)/1 (4)/19 (70)
AR: none/mild/mod-sev, n (%)	9 (33)/3 (11)/15 (56)
Mixed AS and AR (all severities), n (%)	12 (44)
Both mod-sev AS and AR, n (%)	8 (30)
SOV diameter (cm), mean±SD [range]	4.4±0.7 [3.2–5.7]
Mid-AA diameter (cm), mean±SD [range]	4.6±0.5 [3.3–6.3]
Stanford Fazel aortopathy classification	
cluster 1, n (%)	4 (15)
cluster 2, n (%)	8 (30)
cluster 3, n (%)	5 (18)
cluster 4, n (%)	10 (37)
LV SV (mL), mean±SD	105±34
LV EF (%), mean±SD	59±12

SD: standard deviation; BAV: bicuspid aortic valve; BSA: body surface area; ap: anterior-posterior; lat: lateral; RL: right-left coronary sinus; RN: right-non coronary sinus; LN: left-non coronary sinus; AS: aortic stenosis; AR: aortic regurgitation; mod-sev: moderate-severe; SOV: sinus of Valsalva; AA: ascending aorta; LV: left ventricular; SV: stroke volume; EF: ejection fraction.

Table 2

Medial elastic fiber thickness and wall shear stress (WSS) averaged in healthy volunteers and BAV patients. Data stratified between circumferential locations, aortic valve stenosis (AS) and aorta diameter. For each, n denotes the total number of measurements.

Healthy volunteers	**Measurements, n**	**Elastic fiber thickness (μm), median (interquartile range)**	**WSS (Pa), median (interquartile range)**
Anterior wall	40	-	0.55 (0.42–0.73)
Posterior wall	40	-	0.64 (0.55–0.72)
Greater curvature	40	-	0.60 (0.44–0.67)‡
Lesser curvature	40	-	0.63 (0.51–0.84)
All BAV patients			
Anterior wall	25	3.08 (2.72–3.29)	**0.78 (0.62–0.96)**
Posterior wall	23	2.95 (2.67–3.13)	**1.35 (0.88–1.66)** *, ǂ
Greater curvature	30	2.71 (2.56–2.88) *, ‡	**1.20 (0.99–1.38)** *, ǂ
Lesser curvature	15	3.10 (2.93–3.25)	0.77 (0.62–1.02)
BAV subgroups according to aortic valve stenosis (AS)			
AS (AR or no-AR)	73	2.94 (2.67–3.13)	1.10 (0.76–1.46)
no AS (predominant AR)	20	2.76 (2.54–3.16)	0.93 (0.78–1.14)
BAV subgroups according to maximal aorta diameter (cm)			
< 4.5	33	2.94 (2.69–3.20)	0.99 (0.77–1.37)
4.5 – 5	42	2.95 (2.66–3.12)	1.01 (0.77–1.33)
≥ 5	18	2.70 (2.56–3.02)	1.14 (0.78–1.45)

AR: aortic valve regurgitation

* $p<0.05$ for comparison against A;

ǂ against LC regions, within healthy volunteers and patients groups.

Bold numbers indicate $p<0.05$ against healthy volunteers.